TRPM4 Regulates Calcium Oscillations After T Cell Activation

Pierre Launay,[1]*† Henrique Cheng,[2]*‡ Subhashini Srivatsan,[1] Reinhold Penner,[2] Andrea Fleig,[2] Jean-Pierre Kinet[1]§

TRPM4 has recently been described as a calcium-activated nonselective (CAN) cation channel that mediates membrane depolarization. However, the functional importance of TRPM4 in the context of calcium (Ca^{2+}) signaling and its effect on cellular responses are not known. Here, the molecular inhibition of endogenous TRPM4 in T cells was shown to suppress TRPM4 currents, with a profound influence on receptor-mediated Ca^{2+} mobilization. Agonist-mediated oscillations in intracellular Ca^{2+} concentration ($[Ca^{2+}]_i$), which are driven by store-operated Ca^{2+} influx, were transformed into a sustained elevation in $[Ca^{2+}]_i$. This increase in Ca^{2+} influx enhanced interleukin-2 production. Thus, TRPM4-mediated depolarization modulates Ca^{2+} oscillations, with downstream effects on cytokine production in T lymphocytes.

The intensity and shape of Ca^{2+} signals (e.g., oscillations versus sustained Ca^{2+} influx) have been recognized to be essential in setting the threshold for different transcription programs (*1*). This has been particularly well established in the context of T lymphocyte activation and NFAT (nuclear factor of activated T cells)–dependent interleukin-2 (IL-2) production (*2*–*4*). The molecular and electrophysiological characterization of TRPM4 as a Ca^{2+}-activated nonselective (CAN) channel (*5*–*8*) raised the question of its potential role in modulating Ca^{2+}-dependent cellular responses in the physiological context of intact cells. Two splice variants of TRPM4 are known: the short form, TRPM4a (*9*), which lacks 174 amino acid residues at the N terminus; and the long form, TRPM4b (*5*) (referred to here as TRPM4). The latter is a widely expressed CAN channel (*10*, *11*) that does not conduct Ca^{2+} but instead mediates cell membrane depolarization. We hypothesized that the capacity of TRPM4 to depolarize the cells in response to changes in $[Ca^{2+}]_i$ can affect the shape and intensity of Ca^{2+} signals initiated by receptor stimulation, thereby modulating important effector functions such as the transcription programs leading to IL-2 production.

Multimerization of TRPM4 is likely required to form the proper pore structure of the channel. Therefore, we designed a strategy to suppress TRPM4 currents using a dominant negative approach. Inactive monomers of mutants with an intact capacity to multimerize could associate with endogenous channels and generate a dominant negative effect. This would permit the analysis of the role of TRPM4 in effector functions. Two deletion mutants of TRPM4 were generated and analyzed (*12*): deletion of the first 177 amino acids in the N terminus (ΔN-TRPM4) and of the last 160 amino acids in the C terminus (ΔC-TRPM4). The C terminus contains a coil-coiled domain that could be involved in protein-protein interactions (Fig. 1A). The cDNAs corresponding to the Flag-tagged wild-type (wt)-TRPM4 and the two V5-tagged deleted forms were each transfected into a human embryonic kidney 293 (HEK-293) cell line.

Selected stable clones overexpressing either wt-, ΔN-, or ΔC-TRPM4 were assessed for their capacity to localize to the cell surface. The cells were subjected to surface iodination, and the lysates were immunoprecipitated with anti-V5, anti-Flag, and

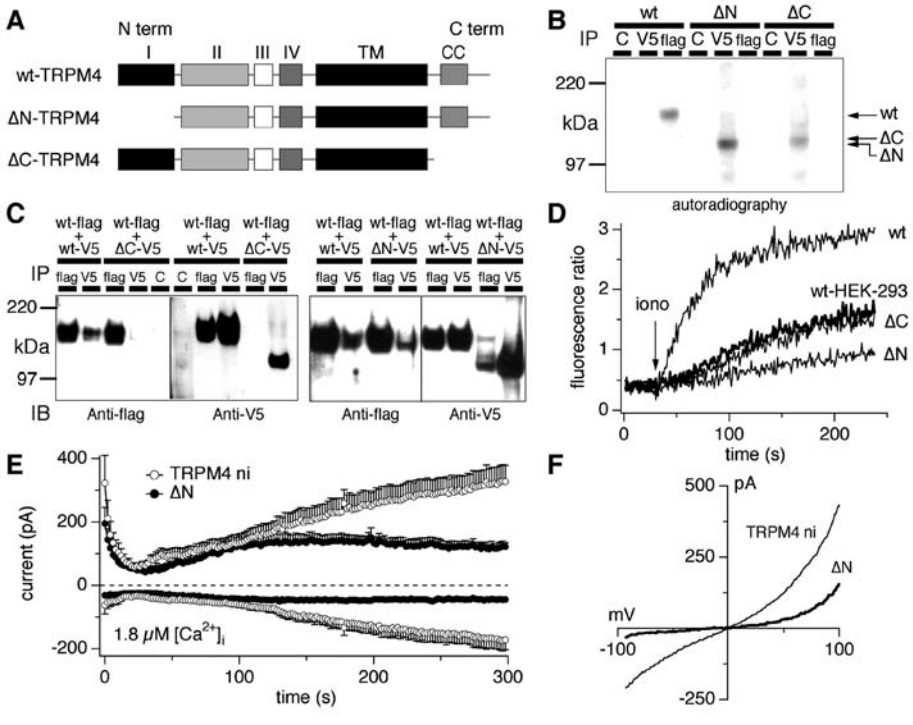

Fig. 1. Structure-function analysis of TRPM4 in HEK-293 cells. (**A**) Schematic representation of wt-TRPM4 and the truncated forms ΔN-TRPM4 and ΔC-TRPM4 with the N-terminal unique regions I to IV, transmembrane domain (TM), and coiled-coil region (CC). (**B**) Surface expression of wt-TRPM4 and the truncated forms. Surface-expressed proteins are labeled with iodine. The wt-TRPM4 molecule was immunoprecipitated with anti-Flag and the two truncated forms, ΔC and ΔN, with anti-V5. (**C**) The C-terminal domain of TRPM4 is involved in its multimerization. HEK-293 cells were cotransfected with two different tagged forms (V5 and Flag) of wt-TRPM4 or cotransfected with Flag-tagged wt-TRPM4 and V5-tagged ΔN-TRPM4 or V5-tagged ΔC-TRPM4. Proteins of cell lysates were immunoprecipitated with Flag and V5, and filters of immune complexes were blotted with both anti-V5 and anti-Flag. (**D**) Na^+ entry following TRPM4 activation by ionomycin (2.5 μM) in intact HEK-293 cell populations loaded with SBFI. Both wild-type HEK-293 cells, as well as cells transfected with ΔC-TRPM4, produced intermediate Na^+ entry, reflecting activity of endogenous TRPM4. Tetracycline-induced cells overexpressing wt-TRPM4 produced larger Na^+ entry, whereas cells expressing the truncated ΔN-TRPM4 form had reduced Na^+ entry. (**E**) Average inward and outward currents at –80 and +80 mV in noninduced (TRPM4 ni) and ΔN-TRPM4–expressing HEK-293 cells stimulated by $[Ca^{2+}]_i$ clamped at 1.8 μM (n = 6 to 7 cells, mean ± SEM). (**F**) *I-V* relationships under the same experimental conditions as in (E), obtained from representative cells 300 s after whole-cell establishment.

isotype control (C) antibodies. Specific antibodies (anti-Flag or anti-V5) precipitated single bands with the predicted molecular sizes (134 kD for wt-TRPM4, 115 kD for ΔN-TRPM4, and 118 kD for ΔC-TRPM4), and no band was seen with the nonspecific or isotype control antibodies (Fig. 1B). These data indicate that both ΔN- and ΔC-TRPM4 are expressed at the plasma membrane.

The ability of ΔN- or ΔC-TRPM4 to heteromultimerize with wt-TRPM4 was assessed by expressing the relevant constructs in HEK-293 cells. Flag-tagged wt-TRPM4 was expressed with either V5-tagged wt-, ΔN-, or ΔC-TRPM4. Flag–wt-TRPM4 was immunoprecipitated in complexes with V5-wt-TRPM4 and with V5-ΔN-TRPM4 but not with V5-ΔC-TRPM4 (Fig. 1C), indicating that monomers of wt-TRPM4 can homomultimerize and that ΔN-TRPM4, but not ΔC-TRPM4, can heteromultimerize with wt-TRPM4. Thus, it appears that the last 160 amino acids of the C-terminal region of TRPM4 may be required for multimerization.

Because the main ion carried by TRPM4 is Na^+, we tested the capacity of the mutant and wt-TRPM4 channels to mediate Na^+ entry in response to an ionomycin-induced elevation in $[Ca^{2+}]_i$ (*12*), using sodium-binding benzofuran isophthalate (SBFI), a specific ratiometric Na^+ dye (*13*, *14*). Ionomycin application induced an increase in $[Na^+]_i$ in wt-HEK-293 cells, presumably through endogenous TRPM4. An even greater increase was observed in cells overexpressing wt-TRPM4 (wt) (Fig. 1D). However, expression of ΔC-TRPM4 did not affect the endogenous cation channels, suggesting that the C terminus is involved in TRPM4 multimerization. In contrast, there was reduced Na^+ entry in cells expressing ΔN-TRPM4, suggesting a dominant negative effect of ΔN-TRPM4 on endogenous TRPM4.

To determine whether the reduction in $[Na^+]_i$ observed in the ΔN-TRPM4–expressing cells was a direct consequence of the inhibition of endogenous TRPM4, we used patch-clamp recordings (*12*) to assess whole-cell membrane currents in noninduced HEK-293 cells and in ΔN-TRPM4 transfectants with $[Ca^{2+}]_i$ clamped at 1.8 μM (Fig. 1E). The noninduced cells generated currents with current-voltage (*I-V*) characteristics similar to those of endogenous TRPM4 described previously (*5*) (Fig. 1F). In contrast, TRPM4 currents in ΔN-TRPM4 transfectants were greatly diminished (Fig. 1, E and F), consistent with the interpretation that ΔN-TRPM4 has a dominant negative effect on endogenous TRPM4 currents.

To determine the function of TRPM4, we examined endogenous channels in immune cells, the cellular responses of which heavily rely on long-lasting oscillatory changes in $[Ca^{2+}]_i$. To assess the endogenous expression of the TRPM4 molecule, we generated a rabbit polyclonal antibody against TRPM4. The antibody recognized V5-wt-TRPM4 by immunoprecipitation and Western blot analysis (*15*). Anti-TRPM4 also detected endogenous TRPM4 protein in HEK-293 cells, in which we originally characterized TRPM4 (*5*) (Fig. 2A). It also recognized TRPM4 in mouse thymocytes, in the mouse Th2 cell clone, D10.G4, and in the two human T lymphoblast cell lines, Molt-4 and Jurkat (Fig. 2B), suggesting that TRPM4 is a conserved and an important ion channel for lymphocytes across multiple species. The antibody reacts specifically with TRPM4, because the single band detected by the antibody disappeared when Jurkat cell lysates were preincubated with the immunizing peptide (Fig. 2C).

Jurkat T cells are a widely used model for the study of Ca^{2+} signaling (*4*, *16*, *17*). Perfusion with 100 to 800 nM $[Ca^{2+}]_i$ revealed concentration-dependent activation of large currents (Fig. 2D). The *I-V* relationships obtained at 200 s after initiation of the experiment for each concentration (Fig. 2E) are consistent with those previously reported for TRPM4. Because TRPM4 is a monovalent-specific cation channel that does not pass any appreciable amount of Ca^{2+}, we assessed whether Na^+ is the main cation responsible for inward currents. When extracellular Na^+ was substituted with isotonic *N*-methyl-D-glucamine chloride (NMDG), almost complete abolition of the inward currents was observed, whereas the outward currents were only slightly reduced. This effect was reversible when NaCl-based Ringer solution was readmitted (Fig. 2F). The *I-V* relationships of

[1]Department of Pathology, Beth Israel Deaconess Medical Center and Harvard Medical School, Boston, MA 02215, USA. [2]Laboratory of Cell and Molecular Signaling, Center for Biomedical Research at The Queen's Medical Center and John A. Burns School of Medicine at the University of Hawaii, Honolulu, HI 96813, USA.

*These authors contributed equally to this work.
†Present address: INSERM E0225, Bichat Medical School, 75870 Paris Cedex 18, France.
‡Present address: All Children's Hospital and University of South Florida, 140 Seventh Avenue South, CRI 2012 St. Petersburg, FL 33701, USA.
§To whom correspondence should be addressed. E-mail: jkinet@bidmc.harvard.edu

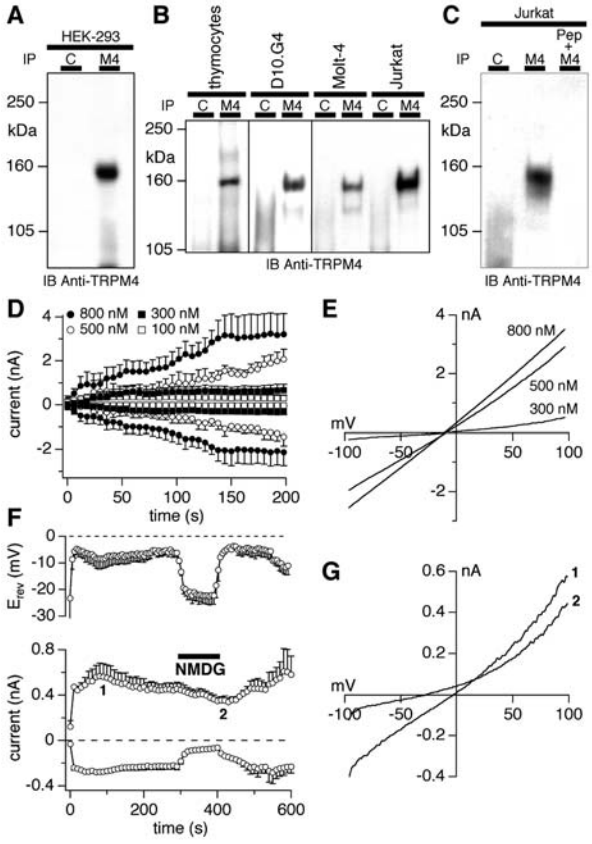

Fig. 2. Characterization of TRPM4 in Jurkat T lymphocytes. (**A**) HEK-293 cells were analyzed for the endogenous expression of TRPM4 protein after immunoprecipitation and immunoblotting with the polyclonal antibody against TRPM4 (M4). Control immunoprecipitation with an irrelevant antibody is indicated by C. (**B**) Detection of endogenous TRPM4 after immunoprecipitation and immunoblotting with anti-TRPM4 in mouse thymocytes and the mouse Th2 clone D10.G4, as well as in the human T cell lines Molt-4 and Jurkat. (**C**) The anti-TRPM4 reactivity is inhibited by preincubation with the peptide. (**D**) Endogenous TRPM4-like currents in Jurkat cells. Average inward and outward currents in wt-Jurkat cells at –80 and +80 mV with $[Ca^{2+}]_i$ clamped at the indicated concentrations (n = 3 to 5 cells, mean ± SEM). (**E**) *I-V* relationship under the same experimental conditions as in (D), obtained from representative cells 200 s after whole-cell establishment. (**F**) (Bottom panel) Average inward and outward currents carried by TRPM4 at –80 and +80 mV, respectively. Cells were perfused with solutions in which $[Ca^{2+}]_i$ was buffered at 800 nM (n = 3 cells, mean ± SEM). For the time indicated, cells were exposed to an isotonic NMDG-Cl–based solution that additionally contained 1 mM $CaCl_2$ and 2 mM $MgCl_2$. The numbers 1 and 2 indicate the time at which raw data traces displayed in (F) were extracted. (Top panel) Reversal potentials extracted from individual ramp current records. (**G**) *I-V* relationships of TRPM4 currents under the same experimental conditions as in (F), measured in a representative cell before (1) and during (2) application of an NMDG-Cl–based solution.

whole-cell currents obtained at the peak of TRPM4 activation and during exposure to NMDG confirm that the reduction in Na^+ influx causes a hyperpolarizing shift in reversal potential (Fig. 2F, top panel, and 2G). Taken together, these data demonstrate that Jurkat cells express functional endogenous CAN channels with the same characteristics as those described previously for TRPM4.

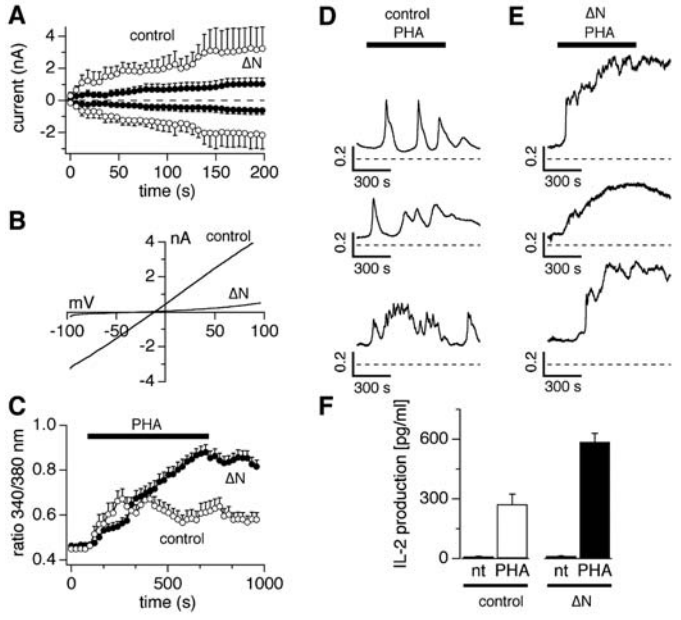

Fig. 3. Structural dissociation of TRPM4 increases receptor-mediated Ca^{2+} entry and IL-2 production. (**A**) Average inward and outward currents in wt-Jurkat and ΔN-TRPM4–expressing cells at −80 and +80 mV with $[Ca^{2+}]_i$ clamped at 800 nM (n = 5 to 6 cells, mean ± SEM). The dominant negative effect of ΔN-TRPM4 is apparent. (**B**) *I-V* relationships under the same experimental conditions as in (A), obtained from representative cells 200 s after whole-cell establishment. (**C**) Average $[Ca^{2+}]_i$ signals from ΔN-TRPM4 (n = 45 cells, 4 experiments) and wt-Jurkat cells (n = 25 cells, 3 experiments) loaded with Fura-2-AM and stimulated with PHA (20 μg/ml). (**D** and **E**) Representative traces of three individual wt-Jurkat and ΔN-TRPM4 Jurkat cells. (**F**) PHA-induced IL-2 production in control wt-Jurkat and ΔN-TRPM4-Jurkat cells. The data shown are the means (±SD) of three independent experiments ($P < 0.004$, unpaired Student's t test).

Clones of Jurkat cells expressing ΔN-TRPM4 were selected, based on protein expression (*15*), and compared to clones expressing the empty vector (control). Cells were perfused with 800 nM $[Ca^{2+}]_i$. Inward currents, obtained at –80 mV after 200 s, in the ΔN-TRPM4 clones were on average ~600 pA, which is smaller than those seen in control cells by a factor of about 3 (Fig. 3, A and B). Thus, the expression of ΔN-TRPM4 has a strong dominant negative effect on endogenous TRPM4 currents in lymphocytes. Conversely, expression of ΔC-TRPM4 in Jurkat cells had no effect on endogenous TRPM4 currents, and these currents were comparable to the ones from clones expressing the empty vector (*15*).

Given that TRPM4 activation would lead to membrane depolarization, we studied the effect of TRPM4 on Ca^{2+} influx in both wt-Jurkat cells and cells in which TRPM4 was suppressed by the ΔN-TRPM4 construct. Average Ca^{2+} signals from ΔN-TRPM4 (n = 45 cells, 4 experiments) and control wt-Jurkat cells (n = 25 cells, 3 experiments) stimulated with phytohemagglutinin (PHA, 20 μg/ml) were determined (Fig. 3C). Representative traces from wt-control cells revealed a pattern of changes in $[Ca^{2+}]_i$ that was characterized by oscillations (Fig. 3D). In ΔN-TRPM4 cells, the oscillatory pattern in $[Ca^{2+}]_i$ was transformed into a prolonged sustained Ca^{2+} influx (Fig. 3E). IL-2 cytokine release by lymphocytes (*12*) is dependent on increases in $[Ca^{2+}]_i$, and IL-2 secretion of PHA-stimulated ΔN-TRPM4 cells was increased 2.2-fold compared with that of the control wt-Jurkat cells (Fig. 3F).

To further evaluate TRPM4 regulation of Ca^{2+} influx in Jurkat T cells and to eliminate possible clonal variations resulting from cellular drug selection, we reduced expression of endogenous TRPM4 using an RNA interference (RNAi) approach (*12*, *18*). About 90 to 95% of Jurkat cells were positively infected as determined with a green fluorescent protein (GFP)–control retroviral vector (*15*). TRPM4-specific siRNA decreased TRPM4 mRNA (Fig. 4A, upper panel) as compared to treatment with a scrambled sequence. There was no decrease in the level of small ribosomal protein (Fig. 4A, lower panel). Immunoprecipitation and Western blot analysis with the polyclonal antibody to TRPM4 (Fig. 4B, upper panel) showed a decrease in TRPM4 protein in the TRPM4 siRNA–infected Jurkat cells. No changes in β-actin protein levels were observed (Fig. 4B, lower panel). Electrophysiology analysis further verified the decrease of TRPM4 currents in TRPM4 siRNA–infected Jurkat cells (Fig. 4, C and D).

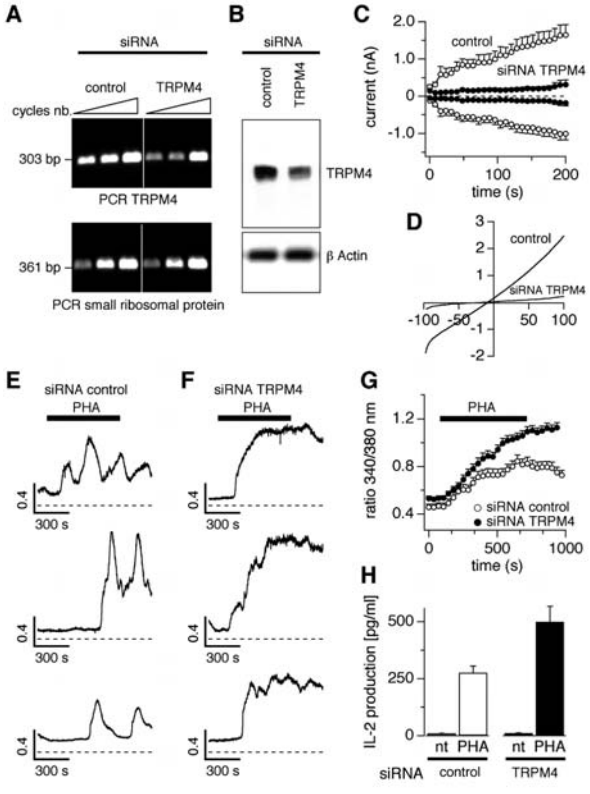

Fig. 4. Gene silencing of TRPM4 increases receptor-mediated Ca^{2+} entry and IL-2 production. (**A**) Reverse transcription–polymerase chain reaction (RT-PCR) of TRPM4 mRNA from Jurkat cells infected with a TRPM4-specific siRNA and a scrambled sequence control. Number of cycles: 32, 34, and 36. Positive control for RT-PCR used primers specific for small ribosomal protein. Number of cycles: 22, 24, and 26. (**B**) Cell lysates were immunoprecipitated with anti-TRPM4 and anti–β-actin and subjected to Western blotting with the same antibodies, respectively. (**C**) Average inward and outward currents in Jurkat cells infected with a TRPM4-specific siRNA (n = 6 ± SEM) and a scrambled sequence control (n = 7 ± SEM) at −80 and +80 mV with $[Ca^{2+}]_i$ clamped at 800 nM. The decrease in current due to the TRPM4 siRNA effect is apparent. (**D**) *I-V* relationships obtained from representative cells 200 s after whole-cell establishment. (**E** and **F**) Representative $[Ca^{2+}]_i$ signals from control siRNA and TRPM4 siRNA Jurkat cells. (**G**) Average Ca^{2+} signals from TRPM4 siRNA (n = 64 cells, 5 experiments) and control siRNA (n = 33 cells, 4 experiments) cells loaded with Fura-2-AM and stimulated with PHA (20 μg/ml). (**H**) PHA-induced IL-2 production in control siRNA and TRPM4 siRNA–infected Jurkat cells. The data shown are the means (±SD) of five independent experiments ($P < 0.017$, unpaired Student's t test).

The siRNA-infected cells were assessed for changes in Ca^{2+} oscillation patterns. Average Ca^{2+} signals from Jurkat cells infected with TRPM4 siRNA (n = 64 cells, 5 experiments) and control siRNA (n = 33 cells, 4 experiments) were determined (Fig. 4G). Jurkat cells infected with TRPM4 siRNA exhibited a more prolonged sustained Ca^{2+} influx as compared to cells infected with the siRNA control, which exhibit oscillatory changes typical of wt-Jurkat cells (compare Fig. 4, E and F). PHA stimulation of these cells resulted in a twofold increase in the amount of IL-2 secreted by the TRPM4 siRNA–infected cells as compared with the amount of IL-2 secreted by the control cells (Fig. 4H).

In summary, our results establish that TRPM4 is a previously unrecognized ion channel in Jurkat T cells with a profound influence on Ca^{2+} signaling. Molecular suppression of TRPM4 converts oscillatory changes of $[Ca^{2+}]_i$ into long-lasting sustained elevations in Ca^{2+} and leads to augmented IL-2 production. It is conceivable that this effect occurs physiologically in cells that express the short splice variant TRPM4a, which is of a similar length to ΔN-TRPM4 and could therefore act as a native dominant negative subunit. In electrically nonexcitable cells, TRPM4 would tend to reduce Ca^{2+} influx by depolarizing the membrane potential and reducing the driving force for Ca^{2+} entry through store-operated CRAC (Ca^{2+} release–activated Ca^{2+}) channels.

The molecular and electrophysiological identification of TRPM4 in Jurkat T cells may call for a reinterpretation of the interplay of ionic currents that shape intracellular Ca^{2+} signals (*4*, *16*, *19*). We propose that TRPM4 acts in concert with CRAC, Kv1.3, and K_{Ca} channels to control $[Ca^{2+}]_i$ oscillations in lymphocytes through oscillatory changes in membrane potential according to the following model.

At rest, the lymphocyte membrane potential is around –60 mV, owing to the basal activity of K^+ channels (*20*). Engagement of T cell receptors induces phospholipase C–mediated production of $InsP_3$ (inositol 1,4, 5-trisphosphate), which causes Ca^{2+} release and activation of store-operated CRAC channels. Current models of Ca^{2+} oscillations in lymphocytes (*19*) propose that the I_{CRAC}-mediated Ca^{2+} influx triggers the activation of Ca^{2+}-activated K^+ channels, which provides the driving force for Ca^{2+} entry by hyperpolarizing the membrane potential until $[Ca^{2+}]_i$ reaches a high-enough level to inhibit I_{CRAC}. As Ca^{2+} entry through I_{CRAC} is reduced, $[Ca^{2+}]_i$ falls until it reaches a level that removes the negative feedback on I_{CRAC}, and the cycle resumes by increasing Ca^{2+} entry through I_{CRAC}. This model lacks a strong depolarizing conductance that would be required to recruit voltage-dependent Kv1.3 channels present in T cells and could account for the observed oscillations in membrane potential (*20*, *21*). The $[Ca^{2+}]_i$-dependent activation of TRPM4 channels may provide this mechanism by becoming activated at around the peak of an oscillatory Ca^{2+} transient, causing the membrane potential to depolarize and thereby substantially reducing the driving force for Ca^{2+} influx. The depolarization would then recruit voltage-dependent K^+ currents (Kv1.3), which would tend to repolarize the membrane potential and also aid in the closure of TRPM4 channels, because the open probability of TRPM4 channels is reduced at negative membrane voltages (*5*, *6*, *8*). The repolarization would reestablish the driving force for Ca^{2+} influx through I_{CRAC} so that the next oscillation in $[Ca^{2+}]_i$ can take place.

References and Notes

1. G. R. Crabtree, *J. Biol. Chem.* **276**, 2313 (2001).
2. R. E. Dolmetsch, K. Xu, R. S. Lewis, *Nature* **392**, 933 (1998).
3. W. Li, J. Llopis, M. Whitney, G. Zlokarnik, R. Y. Tsien, *Nature* **392**, 936 (1998).
4. R. S. Lewis, *Annu. Rev. Immunol.* **19**, 497 (2001).
5. P. Launay *et al.*, *Cell* **109**, 397 (2002).
6. T. Hofmann, V. Chubanov, T. Gudermann, C. Montell, *Curr. Biol.* **13**, 1153 (2003).
7. M. Murakami *et al.*, *Biochem. Biophys. Res. Commun.* **307**, 522 (2003).
8. B. Nilius *et al.*, *J. Biol. Chem.* **278**, 30813 (2003).
9. X. Z. Xu, F. Moebius, D. L. Gill, C. Montell, *Proc. Natl. Acad. Sci. U.S.A.* **98**, 10692 (2001).
10. O. H. Petersen, *Curr. Biol.* **12**, R520 (2002).
11. B. Nilius, G. Droogmans, R. Wondergem, *Endothelium* **10**, 5 (2003).
12. Materials and methods are available as supporting material on *Science* Online.
13. A. T. Harootunian, J. P. Kao, B. K. Eckert, R. Y. Tsien, *J. Biol. Chem.* **264**, 19458 (1989).
14. A. Minta, R. Y. Tsien, *J. Biol. Chem.* **264**, 19449 (1989).
15. P. Launay *et al.*, data not shown.
16. M. D. Cahalan, H. Wulff, K. G. Chandy, *J. Clin. Immunol.* **21**, 235 (2001).
17. R. T. Abraham, A. Weiss, *Nat. Rev. Immunol.* **4**, 301 (2004).
18. T. R. Brummelkamp, R. Bernards, R. Agami, *Science* **296**, 550 (2002).
19. R. E. Dolmetsch, R. S. Lewis, *J. Gen. Physiol.* **103**, 365 (1994).
20. J. A. Verheugen, H. P. Vijverberg, *Cell Calcium* **17**, 287 (1995).
21. C. M. Fanger *et al.*, *J. Biol. Chem.* **276**, 12249 (2001).

22. We thank M. K. Monteilh-Zoller and C. E. Oki for technical assistance, L. Glimcher's laboratory for providing the murine T cell clone D10.G4, and S. Kraft for insightful advice on the RNAi method. This work was supported in part by NIH grants R01-AI46734 (J.-P.K.); R01-NS40927, R01-AI50200, and R01-GM63954 (R.P.); and R01-GM65360 (A.F.). P.L. was supported by a fellowship from the Human Frontier Science Program Organization.

Supporting Online Material

www.sciencemag.org/cgi/content/full/306/5700/1374/DC1
Materials and Methods

6 April 2004; accepted 14 September 2004

A Protein Sensor for siRNA Asymmetry

Yukihide Tomari, Christian Matranga, Benjamin Haley, Natalia Martinez, Phillip D. Zamore*

To act as guides in the RNA interference (RNAi) pathway, small interfering RNAs (siRNAs) must be unwound into their component strands, then assembled with proteins to form the RNA-induced silencing complex (RISC), which catalyzes target messenger RNA cleavage. Thermodynamic differences in the base-pairing stabilities of the 5′ ends of the two ~21-nucleotide siRNA strands determine which siRNA strand is assembled into the RISC. We show that in *Drosophila*, the orientation of the Dicer-2/R2D2 protein heterodimer on the siRNA duplex determines which siRNA strand associates with the core RISC protein Argonaute 2. R2D2 binds the siRNA end with the greatest double-stranded character, thereby orienting the heterodimer on the siRNA duplex. Strong R2D2 binding requires a 5′-phosphate on the siRNA strand that is excluded from the RISC. Thus, R2D2 is both a protein sensor for siRNA thermodynamic asymmetry and a licensing factor for entry of authentic siRNAs into the RNAi pathway.

In *Drosophila* lysates, siRNAs are loaded into the RISC by an ordered pathway in which one of the two siRNA strands, the guide strand, is assembled into the RISC, whereas the other strand, the passenger strand, is excluded and destroyed (*1*–*14*). A central step in RISC assembly is formation of the RISC-loading complex [RLC, previously designated complex A (*13*)], which contains double-stranded siRNA, the double-stranded RNA binding protein R2D2, and Dicer-2 (Dcr-2), as well as additional unidentified proteins. The function of Dicer in loading siRNA into the RISC is distinct from its role in generating siRNA from long double-stranded RNA (dsRNA) (*10*, *15*). Both R2D2 and Dcr-2 are

Department of Biochemistry and Molecular Pharmacology, University of Massachusetts Medical School, Worcester, MA 01605, USA.

*To whom correspondence should be addressed. E-mail: phillip.zamore@umassmed.edu